

# Accepted Manuscript

Research paper

Syntheses, solid structures, and behavior in solution of  $[\text{Ml}_2(\text{CO})_3(\text{pyrazole})_2]$  complexes (M = Mo, W)

Paloma Paredes, Fernando Lorenzo, Sonia Bajo, Elena Cuéllar, Carsten Strohmann, Jose M. Martín-Alvarez, Daniel Miguel, Fernando Villafañe

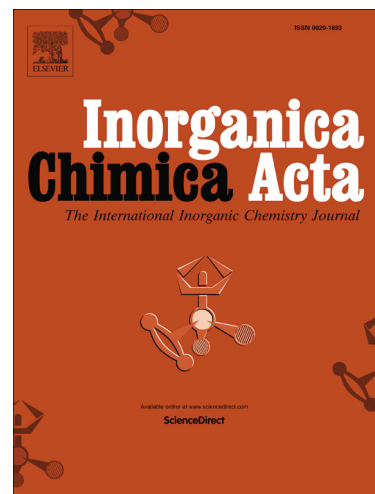
PII: S0020-1693(16)30643-0  
DOI: <http://dx.doi.org/10.1016/j.ica.2016.11.004>  
Reference: ICA 17344

To appear in: *Inorganica Chimica Acta*

Received Date: 4 October 2016  
Revised Date: 3 November 2016  
Accepted Date: 10 November 2016

Please cite this article as: P. Paredes, F. Lorenzo, S. Bajo, E. Cuéllar, C. Strohmann, J.M. Martín-Alvarez, D. Miguel, F. Villafañe, Syntheses, solid structures, and behavior in solution of  $[\text{Ml}_2(\text{CO})_3(\text{pyrazole})_2]$  complexes (M = Mo, W), *Inorganica Chimica Acta* (2016), doi: <http://dx.doi.org/10.1016/j.ica.2016.11.004>

This is a PDF file of an unedited manuscript that has been accepted for publication. As a service to our customers we are providing this early version of the manuscript. The manuscript will undergo copyediting, typesetting, and review of the resulting proof before it is published in its final form. Please note that during the production process errors may be discovered which could affect the content, and all legal disclaimers that apply to the journal pertain.



Submitted to *Inorganica Chimica Acta*

## Syntheses, solid structures, and behavior in solution of [MI<sub>2</sub>(CO)<sub>3</sub>(pyrazole)<sub>2</sub>] complexes (M = Mo, W)

Paloma Paredes,<sup>a</sup> Fernando Lorenzo,<sup>a</sup> Sonia Bajo,<sup>a</sup> Elena Cuéllar,<sup>a</sup> Carsten Strohmann,<sup>b</sup> Jose M. Martín-Alvarez,<sup>a</sup> Daniel Miguel,<sup>a</sup> and Fernando Villafañe<sup>\*,a</sup>

<sup>a</sup> GIR MIOMeT-IU Cinquima-Química Inorgánica, Facultad de Ciencias, Campus Miguel Delibes, Universidad de Valladolid, 47011 Valladolid, Spain.

<sup>b</sup> Anorganische Chemie, Technische Universität Dortmund, Otto-Hahn-Straße 6, 44227 Dortmund, Germany.

*Keywords:*

Pyrazole, Molybdenum, Tungsten, Fluxionality, Isomers

### ABSTRACT

[MI<sub>2</sub>(CO)<sub>3</sub>(pz\*H)<sub>2</sub>] complexes (M = Mo, W; pz\*H = pzH, dmpzH, indzH) have been synthesized and characterized in solid state and in solution. These heptacoordinated complexes present a capped octahedron geometry in the solid state where the azole ligands are always coordinated pseudo-*cis*, and the iodido ligands are coordinated either pseudo-*trans* (pzH complexes and molybdenum complex with indzH) or pseudo-*cis* (tungsten complex with dmpzH). Both isomers are found in the crystal structure of [WI<sub>2</sub>(CO)<sub>3</sub>(indzH)<sub>2</sub>]. The difference in energies between both isomers have been theoretically calculated and range between -2.9 and +1.0 Kcal/mol. The complexes where the iodido ligands are coordinated pseudo-*trans* show unequivalent azoles in the NMR at low temperature while they undergo a dynamic process in solution which

\* Corresponding author. Tel.: +34 983 184620; fax: ++34 983 423013.  
E-mail address: fervilla@qi.uva.es (F. Villafañe).

makes both heterocycles equivalent at room temperature. The other complexes display a dynamic behavior in solution where both heterocycles are equivalent both at room and at low temperatures.

## 1. Introduction

The promising aspects of bis(pyrazole) complexes are based on their structures and reactivity. Concerning their structures, the N-bound hydrogen of pyrazole complexes is usually involved in hydrogen bonds. This fact is related to one of the big challenges of chemistry, i.e. understanding and control of the organization of molecules [1].

Concerning their reactivity, terminal pyrazole ligands are ready useful precursors for bridging pyrazolate homo- or heterobimetallic complexes. These processes occur after deprotonation of the N-bound hydrogen of the coordinated pyrazole if a second metallic substrate is present. This strategy has been successively used by different groups, mainly with middle and late transition elements. However, only a couple of heterobimetallic complexes including group 6 metals with bridging pyrazolates have been so far described [2].

We consider of interest the synthesis of new systems able to generate heterobimetallic systems. The presence in the same molecule of two or more different metals usually enhance its physical and chemical properties, compared to those displayed by the corresponding homonuclear species. This cooperative or synergistic effect has already allowed to obtain new systems catalytically more efficient, or new electronic materials, for example [3].

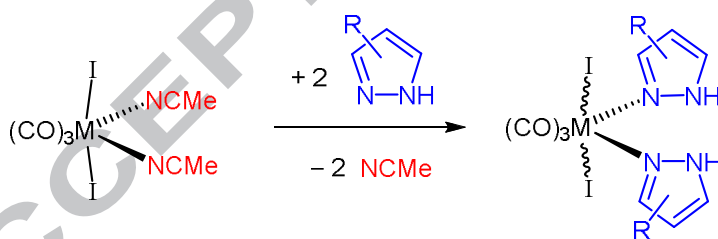
Obviously, molybdenum or tungsten pyrazole complexes might be good precursors for the synthesis of new heterobimetallic complexes containing group 6 metals. However the references on Mo(II) or W(II) complexes with terminal pyrazole ligands are relatively scarce [2b,4]. Following our previous reports on the synthesis, structure, dynamic behavior in solution, and reactivity of bis(pyrazole) complexes of different metals [2b,4g,4h,4i,5]. we herein describe new heptacoordinated  $[M_2(CO)_3(pz^*H)_2]$  complexes (M = Mo, W;  $pz^*H$  = pyrazole, pzH; 3,5-dimethylpyrazole, dmpzH; indazole, indzH). Research on heptacoordinated complexes is somehow limited due to the limitations associated to the characterization of the complexes, what is a consequence of the small differences of energy between the

possible geometries. Besides, most of the heptacoordinated complexes reported show a dynamic behavior in solution, what makes even more difficult their complete characterization [6].

## 2. Results and discussion

### 2.1. Syntheses of the complexes

The complexes were synthesized from the reactions of the bis(acetonitrile) precursors  $[\text{Ml}_2(\text{CO})_3(\text{NCMe})_2]$  ( $\text{M} = \text{Mo}, \text{W}$ ) with the corresponding pyrazole (pzH, dmpzH, indzH) in a 1/2 ratio (Scheme 1). All the reactions, where the pyrazoles substitute the acetonitrile ligands, are fast and occur in  $\text{CH}_2\text{Cl}_2$  at  $0\text{ }^\circ\text{C}$  in 5 min. giving the corresponding disubstituted complexes  $[\text{Ml}_2(\text{CO})_3(\text{pz}^*\text{H})_2]$  ( $\text{M} = \text{Mo}$ ,  $\text{pz}^*\text{H} = \text{pzH}$ , **1**; dmpzH, **2**; indzH; **3**;  $\text{M} = \text{W}$ ,  $\text{pz}^*\text{H} = \text{pzH}$ , **4**; dmpzH, **5**; indzH; **6**). The new compounds are isolated as microcrystalline solids, their colors ranging from orange to brown-red. The starting materials and the new complexes display the three C-O characteristic stretching bands expected for *fac*-tricarbonyl complexes, and therefore the reactions can be monitored by solution IR. These absorptions are also observed in the solid state IR spectra, as well as other typical N-H, and C=N bands of pyrazole ligands (see Experimental). The syntheses and partial characterization of complexes **1** and **4** had been previously reported [7].



**Scheme 1.** Syntheses of the pyrazole complexes **1-6** ( $\text{M} = \text{Mo}, \text{W}$ ; pyrazole = pzH, dmpzH, indzH).

### 2.2. Solid-state structures

Five of the six complexes synthesized were subjected to X-ray diffractive studies. All the attempts to obtain suitable crystals for compound **2** were unsuccessful.

Complexes **1**, **3**, and **4** display a similar structure. They are shown in Figures 1, 2, and 3 respectively, with selected distances and angles included. Details of the whole

structure determination can be found in the CIF. The geometry of the three complexes may be described as a capped octahedron. For **1** (Figure 1), CO(1) occupies the center of the triangular capped face, which is formed by CO(2), CO(3) and I(1). Thus, the angles between the capping ligand and those forming the triangular face are 69.51(13) for C(1)-Mo(1)-I(1), 71.52(17) for C(1)-Mo(1)-C(2), and 72.3(2) for C(1)-Mo(1)-C(3), whereas those between the latter are larger [110.69(12) for C(2)-Mo(1)-I(1), 114.42(12) for C(3)-Mo(1)-I(1), and 104.75(18) for C(3)-Mo(1)-C(2)]. The opposite triangular face of the octahedron is occupied by the second iodine atom I(2) and by both donor nitrogen atoms of the pzH ligands, N(1) and N(3). As expected, the angles between these ligands are shorter than those found at the opposite triangular face: 87.69(9) for N(1)-Mo(1)-I(2), 82.59(12) for N(1)-Mo(1)-N(3), and 88.23(8) for N(3)-Mo(1)-I(2). The rest of the structures therein reported display similar angles, thus allowing to recognize which ligand is in the capped position.

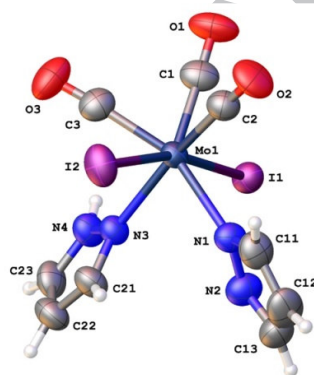


**Figure 1.** Perspective view of  $[\text{MoI}_2(\text{CO})_3(\text{pzH})_2]$ , **1**, showing the atom numbering. Thermal ellipsoids are drawn at 50% probability. Selected bond lengths (Å) and angles (°): Mo(1)-N(1) 2.253(3), Mo(1)-N(3) 2.254(3), Mo(1)-I(2) 2.8397(8), Mo(1)-I(1) 2.8763(8), N(1)-Mo(1)-N(3) 82.59(12), N(1)-Mo(1)-I(2) 87.68(9), N(3)-Mo(1)-I(2) 88.22(8), N(1)-Mo(1)-I(1) 81.01(9), N(3)-Mo(1)-I(1) 81.40(8), I(2)-Mo(1)-I(1) 165.514(17).

In the three structures both iodido ligands are coordinated in a pseudo-*trans* arrangement [8] [for **1**, I(2)-Mo(1)-I(1) 165.514(17)°], as occurs for other structures of complexes  $[\text{MX}_2(\text{CO})_3\text{L}_2]$  (M = Mo, W; X = halogen; L = monodentate N-donor ligand) previously reported [9]. This contrasts with the pseudo-*cis* arrangement for the halido ligands found when only one of the monodentate L ligands is a N-donor [9d,10], or when both L are monodentate P-donor [11]. The pyrazole ligands are coordinated in a

pseudo-*cis* arrangement in the three crystal structures [for **1**, N(1)-Mo(1)-N(3) 82.59(12)°].

In **1**, the N-bound hydrogen of one of the pzH ligands is involved in hydrogen bonding with a iodido ligand of an adjacent molecule. From the distances and angles detected [H(4)⋯I(1) 2.692(1) Å, N(4)⋯I(1) 3.678(1) Å, N(4)-H(4)⋯I(1) 160.25(2)°], it may be considered as a "weak" hydrogen bond [12].

In the crystal structure of **3** (Figure 2), CO(2) is coordinated at the center of the triangular capped face, formed by CO(1), CO(3) and I(2). The second iodine atom I(1) and both donor nitrogen atoms of the indzH ligands, N(1) and N(3) define the opposite triangular face of the octahedron. As for **1**, and for the rest of [MX<sub>2</sub>(CO)<sub>3</sub>L<sub>2</sub>] (M = Mo, W; X = halogen; L = monodentate N-donor ligand) complexes [9], both iodido ligands are coordinated in a pseudo-*trans* arrangement [I(2)-Mo(1)-I(1) 166.29(2)°], whereas the indzH ligands are coordinated pseudo-*cis* [N(1)-Mo-N(3) 82.43(18)°].

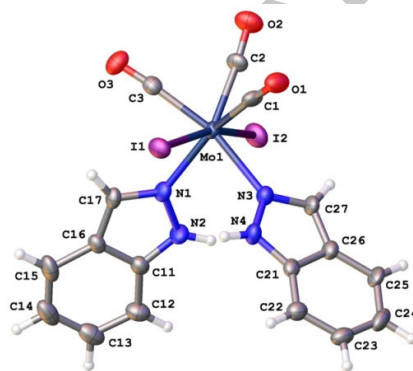


**Figure 2.** Perspective view of [MoI<sub>2</sub>(CO)<sub>3</sub>(indzH)<sub>2</sub>], **3**, showing the atom numbering. Thermal ellipsoids are drawn at 50% probability. Selected bond lengths (Å) and angles (°): Mo-N(3) 2.249(5), Mo-N(1) 2.270(5), Mo-I(2) 2.8493(6), Mo-I(1) 2.8527(6), N(1)-Mo-N(3) 82.48(18), N(1)-Mo-I(2) 82.25(13), N(3)-Mo-I(2) 82.66(12), N(1)-Mo-I(1) 91.52(13), N(3)-Mo-I(1) 84.45(12), I(2)-Mo-I(1) 166.31(2).

The N-bound hydrogen of one of the indzH ligands is involved in hydrogen bonding with a iodido ligand of an adjacent molecule. From the distances and angles detected [H(4)⋯I(2) 2.881(1) Å, N(4)⋯I(2) 3.738(5) Å, N(4)-H(4)⋯I(2) 141.0(3)°], it may be considered as a "weak" hydrogen bond [12].

Figure 3 shows the crystal structure of the tungsten complex **4**, where CO(2) occupies the center of the triangular capped face, which is formed by CO(1), CO(3) and I(2). The opposite triangular face of the octahedron is defined by the second iodine atom I(1), and by both donor nitrogen atoms of the pzH ligands, N(1) and N(3). Again, both

iodido ligands are coordinated in a pseudo-*trans* arrangement [I(2)-W(1)-I(1) 164.14(2)], and both pzH ligands are coordinated pseudo-*cis* [N(1)-W(1)-N(3) 81.6(2)°].

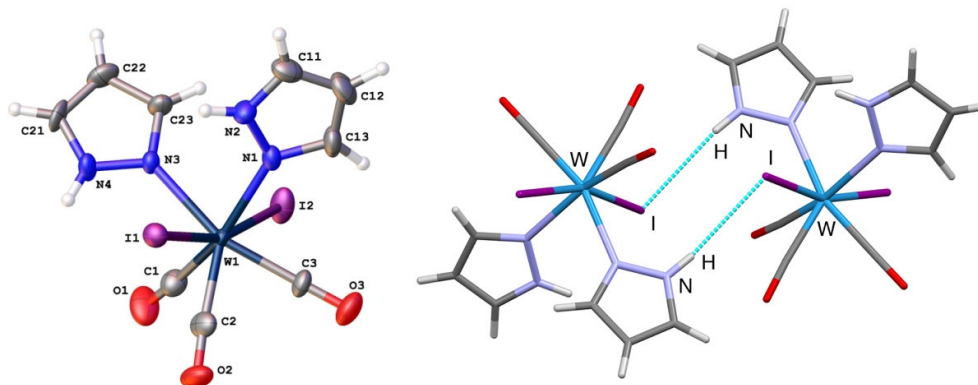


**Figure 3.** (Left) Perspective view of  $[\text{Wl}_2(\text{CO})_3(\text{pzH})_2]$ , **4**, showing the atom numbering. Thermal ellipsoids are drawn at 50% probability. Selected bond lengths (Å) and angles (°): W(1)-N(1) 2.242(6), W(1)-N(3) 2.243(6), W(1)-I(2) 2.8343(10), W(1)-I(1) 2.8647(11), N(1)-W(1)-N(3) 81.6(2), N(1)-W(1)-I(2) 87.08(16), N(3)-W(1)-I(2) 87.27(14), N(1)-W(1)-I(1) 80.91(15), N(3)-W(1)-I(1) 80.79(14), I(2)-W(1)-I(1) 164.14(2). (Right) Perspective view of **4** showing the H bonds between adjacent molecules.

In **4**, the N-bound hydrogen of one of the pzH ligands is involved in hydrogen bonding with a iodido ligand of an adjacent molecule (Figure 3, right). From the distances and angles detected [H(4)⋯I(1) 2.699(1) Å, N(4)⋯I(1) 3.687(6) Å, N(4)-H(4)⋯I(1) 160.7(4)°], it may be considered again as a "weak" hydrogen bond [12].

The crystal structure of **5** (Figure 4) is different from those just described above, since both iodido ligands are coordinated in a pseudo-*cis* arrangement. This is the most striking feature of the structure since, as indicated above, the  $[\text{MX}_2(\text{CO})_3\text{L}_2]$  (M = Mo, W; X = halogen; L = monodentate N-donor ligand) structures previously reported present a pseudo-*trans* arrangement of the two halido ligands [9].

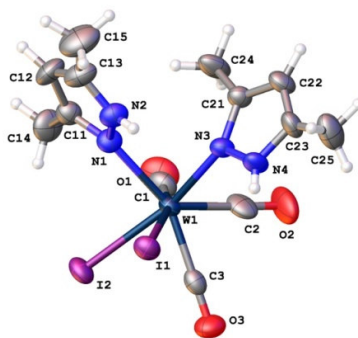


**Figure 4.** Perspective view of  $[\text{Wl}_2(\text{CO})_3(\text{dmpzH})_2]$ , **5**, showing the atom numbering. Thermal ellipsoids are drawn at 50% probability. Selected bond lengths ( $\text{\AA}$ ) and angles ( $^\circ$ ):  $\text{W}(1)\text{-N}(3)$  2.249(6),  $\text{W}(1)\text{-N}(1)$  2.261(6),  $\text{W}(1)\text{-I}(2)$  2.8438(11),  $\text{W}(1)\text{-I}(1)$  2.9063(11),  $\text{N}(3)\text{-W}(1)\text{-N}(1)$  78.4(2),  $\text{N}(3)\text{-W}(1)\text{-I}(2)$  163.62(15),  $\text{N}(1)\text{-W}(1)\text{-I}(2)$  88.27(15),  $\text{N}(3)\text{-W}(1)\text{-I}(1)$  83.01(14),  $\text{N}(1)\text{-W}(1)\text{-I}(1)$  84.53(15),  $\text{I}(2)\text{-W}(1)\text{-I}(1)$  86.29(3).

The geometry of **5** may be again described as a capped octahedron. In this case, CO(2) is coordinated at the center of the triangular capped face, formed by the other two carbonyl atoms, CO(1), CO(3), and by a nitrogen donor atom of one of the dmpzH ligands, N(3). The opposite triangular face of the octahedron is occupied by the donor nitrogen atoms of the second dmpzH ligand, N(1), and by both iodine atoms. As in the previous structures, the dmpzH ligands are coordinated in a pseudo-*cis* arrangement [ $\text{N}(3)\text{-W}(1)\text{-N}(1)$  78.4(2) $^\circ$ ].

Surprisingly, the crystal structure determination of **6** reveals the presence of the two possible isomers, considering the pseudo-*cis* and pseudo-*trans* arrangements of the two iodido ligands, whereas the pseudo-*cis* arrangement of the indazole ligands and the capped octahedron for the heptacoordinated tungsten(II) is maintained in both structures. They are shown in Figure 5 with selected distances and angles.

The geometry in both isomers may be described as a capped octahedron. For the pseudo-*trans* isomer, CO(2) occupies the center of the triangular capped face, which is formed by CO(1), CO(3) and I(2). The opposite triangular face of the octahedron is occupied by the second iodine atom I(1) and by both donor nitrogen atoms of the indzH ligands, N(1) and N(3). For the pseudo-*cis* isomer, CO(52) is coordinated at the center of the triangular capped face, which is defined by the other two carbonyl atoms, CO(51), CO(53), and a nitrogen donor atom of one of the indzH ligands, N(53). The opposite triangular face of the octahedron is formed by the donor nitrogen atoms of the second indzH ligand, N(51), and by both iodine atoms.

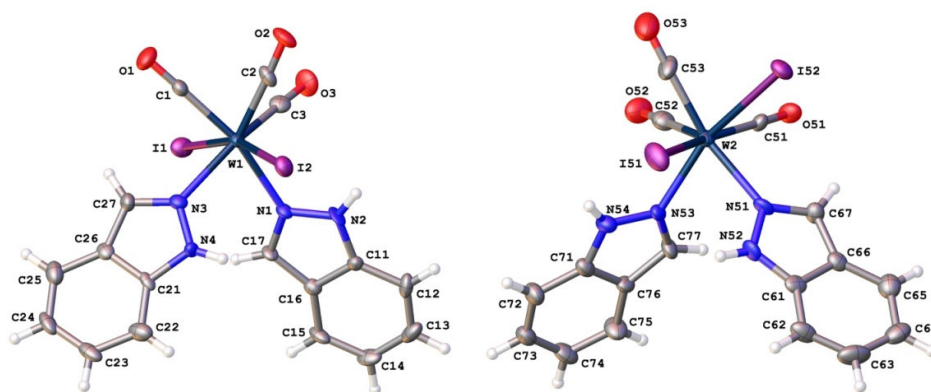


**Figure 5.** Perspective views of the two isomers of  $[Wl_2(CO)_3(indzH)_2]$  (left, pseudo-*trans*, right pseudo-*cis*, **6**, showing the atom numbering. Thermal ellipsoids are drawn at 50% probability. Selected bond lengths (Å) and angles (°): Pseudo-*trans* isomer: W(1)-N(3) 2.256(6), W(1)-N(1) 2.258(6), W(1)-I(1) 2.8353(6), W(1)-I(2) 2.8936(6), N(3)-W(1)-N(1) 82.8(2), N(3)-W(1)-I(1) 82.79(16), N(1)-W(1)-I(1) 88.54(16), N(3)-W(1)-I(2) 81.97(16), N(1)-W(1)-I(2) 80.41(15), I(1)-W(1)-I(2) 162.166(18). Pseudo-*cis* isomer: W(2)-N(53) 2.228(6), W(2)-N(51) 2.242(6), W(2)-I(52) 2.8303(6), W(2)-I(51) 2.8525(6), N(53)-W(2)-N(51) 77.1(2), N(53)-W(2)-I(52) 160.50(15), N(51)-W(2)-I(52) 85.84(15), N(53)-W(2)-I(51) 82.35(16), N(51)-W(2)-I(51) 87.08(15), I(52)-W(2)-I(51) 87.379(17).

As indicated above, both isomers differ on the arrangement of the iodido ligands, the angle I(2)-W(1)-I(1) being  $162.166(18)^\circ$  for the pseudo-*trans* isomer, and I(52)-W(2)-I(51)  $87.379(17)^\circ$  for the pseudo-*cis* isomer. The indzH ligands are coordinated in a pseudo-*cis* arrangement [N(1)-W(1)-N(3)  $82.8(2)^\circ$  for the pseudo-*trans* isomer, and N(51)-W(2)-N(53)  $77.1(2)^\circ$  for the pseudo-*cis* isomer], as for the rest of structures herein reported.

In none of the N-bound hydrogen of the indzH ligands of any of the isomers is involved in hydrogen bonding.

### 2.3. Computational studies

All the complexes were studied theoretically by means of density functional theory (DFT) calculations. The ground-state geometry was optimized at the B3LYP level with no symmetry restraints for all the complexes, using the LANL2DZ basis set with its corresponding ECP for Mo, W and I atoms, and the 6-31G(d,p) basis set for the rest. The optimized geometry compares well with the structure obtained by X-ray diffraction when available. For instance, in compound **1** the difference in bond distances (optimized geometry - experimental geometry) between the Mo atom and the ligand

donor atoms, range from 0.014 Å for Mo-C(2) distance to 0.205 Å for Mo-I(1), and the difference in angles is also small (0.6° for the I(1)-Mo-I(2) angle, or 2.5° for N(1)-Mo-N(3)). The optimized geometry can be slightly improved by using a larger basis set (aug-cc-pVTZ-PP for the Mo and I atoms), but the difference in the energy of the isomers does not change significantly (see below).

In order to rationalize the geometries found in the crystal structures, they are depicted in Figure 6 as trigonal antiprisms to better show the capped face. As described above, complexes **1**, **3**, and **4** display similar solid crystal structures, where one of the carbonyls occupies the center of the triangular capped face, which is formed by the other two carbonyls and by one of the iodido ligands. The opposite triangular face of the octahedron is occupied by the second iodido ligand, so as both iodine atoms are coordinated pseudo-*trans*, and by both donor nitrogen atoms of the azole ligands, which are coordinated respectively pseudo-*cis*. This geometry is labeled *S*, from symmetric, as the geometry has a symmetry plane containing the metal, both iodine atoms and the carbonyl in the capped position.

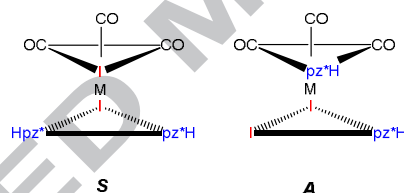


**Figure 6.** Geometries found for the complexes herein described: *S* (symmetric) for **1**, **3**, **4**, and **6** (left); and *A* (asymmetric) for **5**, and **6** (right).

On the other hand, in the crystal structure of complex **5** one of the carbonyls occupies the center of the triangular capped face, which is formed by the other two carbonyl atoms, and a nitrogen donor atom of one of the dmpzH ligands. The opposite triangular face of the octahedron is occupied by the donor nitrogen atoms of the second dmpzH ligand, and by both iodine atoms. Therefore both dmpzH ligands are coordinated relatively pseudo-*cis*, as well as both iodine atoms. This geometry is schematically depicted in Figure 6, and is labeled *A* from asymmetric, as this geometry does not present any symmetry elements.

Table 1 collects the differences in the theoretically calculated energies between isomers *S* and *A* in Kcal/mol with the B3LYP//LANL2DZ/6-31G(d,p) level of theory. Using a larger basis set for the heavy atoms (aug-cc-pVTZ-PP for the Mo and I atoms)

the difference  $E_{(S)}-E_{(A)}$  for compound **1** is  $-1.5$  Kcal/mol, which is very close to the value showed in Table 1 ( $-1.9$  Kcal/mol) and, therefore, we decided to perform all the calculations with the smaller basis set to keep a reasonable computational cost. Two conclusions may be drawn from these data. First, the most stable complex is that found in the crystal structure in all the cases, except for **6**, where both isomers are found in the crystal structure. Second, the values found are really small, as previously reported for other studies on differences of energy between the possible geometries in heptacoordinated complexes [6]. Therefore, trying to establish clear rules about which would be the preferred geometry for a given complex is so far a target out of reach. This also affects to the behavior in solution of these complexes, which is discussed next.

**Table 1.** Differences in the calculated energies between isomers S and A in Kcal/mol.

Compound	$E_{(S)}-E_{(A)}$
$[\text{MoI}_2(\text{CO})_3(\text{pzH})_2]$ , <b>1</b>	$-1.9$
$[\text{MoI}_2(\text{CO})_3(\text{dmpzH})_2]$ , <b>2</b>	$+0.2$
$[\text{MoI}_2(\text{CO})_3(\text{indzH})_2]$ , <b>3</b>	$-2.9$
$[\text{WI}_2(\text{CO})_3(\text{pzH})_2]$ , <b>4</b>	$-1.0$
$[\text{WI}_2(\text{CO})_3(\text{dmpzH})_2]$ , <b>5</b>	$+1.3$
$[\text{WI}_2(\text{CO})_3(\text{indzH})_2]$ , <b>6</b>	$-1.7$

#### 2.4. Behavior in solution

The NMR spectra, recorded at room temperature and at  $-80^\circ\text{C}$ , show dynamic behavior in solution for all the complexes. As in other terminal pyrazole complexes previously reported [3,5], the broadness observed at room temperature for the NH protons signal might be due to a rapid prototropic exchange involving this proton. The unambiguous assignment of the hydrogens (for pzH) or methyl groups (for dmpzH) in positions 3 and 5 is difficult, since their chemical shift seems to be affected by different factors, which are difficult to evaluate, since their resonances may vary in the same family of complexes [13], or even depending on the solvent used [14]. For these fluxional complexes the broader signals have been assigned to the group (H or Me) at position 3, as they are closer to the nonequivalence source than those at position 5, which point to the outside of the complex. Thus, the assignment proposed in the Experimental may be considered as tentative.

The dynamic behavior in solution of heptacoordinated complexes has been recently reviewed by one of us [6], and one of the general conclusions reached therein is that the dynamic processes are so diverse that finding a regular pattern is a very difficult task. For heptacoordinated complexes with a capped octahedron geometry, the exchange processes so far reported include both scrambling and migration of ligands. These processes do not occur on preferential positions in the capped octahedron geometry, but all the coordination sites are involved. On the other hand, the nature of these processes do not seem to depend on the type of ligands present. In addition, their energies are usually rather similar and the dynamic processes often occur simultaneously [6]. Therefore, the precedents found in the literature preclude the unambiguous proposal of a geometry for the isomer found at low temperature, or about the nature of the exchange mechanism. Considering this, the study carried out for the complexes herein described can not be definitely conclusive.

We will consider first the pyrazole complexes **1** and **4**, and the indazole molybdenum complex **3**, which show the same crystal structure (*S* in Figure 6) and the same dynamic behavior in solution: both heterocycles are equivalent at room temperature, and nonequivalent at low temperature (see Figure 7 and Experimental). For **3**, two isomers are found in solution, and that found in the solid state is the major one, as supported by the spectrum obtained from a freshly prepared solution after mixing the solid and frozen solvent.

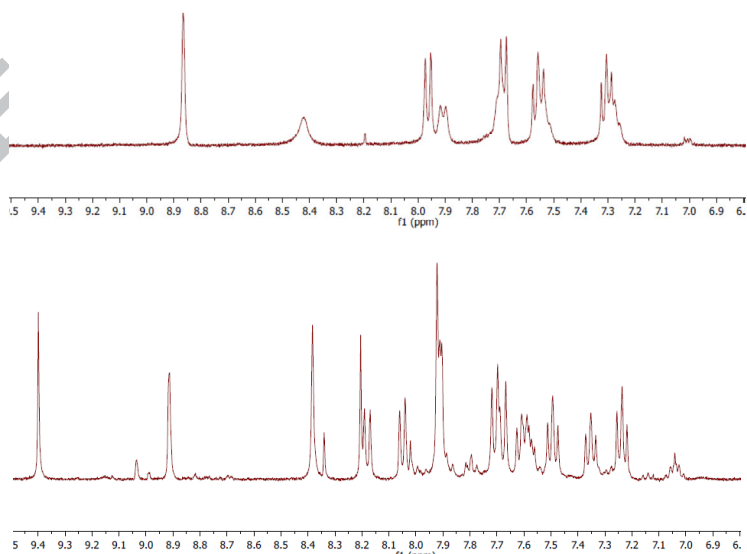


**Figure 7.**  $^1\text{H}$  NMR spectra (aromatic region) of complex  $[\text{MoI}_2(\text{CO})_3(\text{indzH})_2]$ , **3**, at room temperature (above) and at 193 K (below)

These three complexes display geometry *S* in Figure 6. In this geometry, both azoles are equivalent in solution, and this is what is observed at room temperature. However, at low temperature the nitrogen donor ligands became inequivalent, but we should assume that when the dynamic process is fast enough (at room temperature), we observe a symmetric average spectrum.

The simplest proposal which accounts for the experimental observations in the low temperature solutions of **1**, **3**, and **4** would be the restraint of the tilting movement of the pyrazole ligands around the M-N edges (Figure 8). The structure more stable, as has also been theoretically justified, should be that found in the crystal structure, and therefore we may assume that this is the geometry which occurs at low temperatures. In this geometry, if the tilting movement of the pyrazole ligands around the M-N edge had been restrained, the pyrazoles would be inequivalent, as well as each half of the pyrazole (i.e. C<sup>3</sup>H vs. C<sup>5</sup>H in pyrazole). This is observed in the low temperature spectra. At room temperature, the fast tilt movement around the M-N edge would make both pyrazoles equivalent, given the symmetry plane containing the metal, both iodine atoms and the carbonyl in the capped position. The energy of this movement is supposed to be very low, but any other proposal to explain this dynamic behavior contrasts with the fact that the structure found in the crystal should be the more stable, and with the symmetric geometry of the molecule.

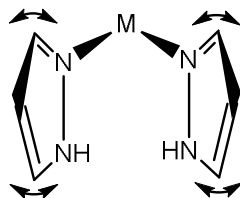


**Figure 8.** Tilting movement of the pyrazole ligands around the M-N edges

The dmpzH complexes **2** and **5** display similar dynamic behavior in solution, although different from that just described for **1**, **3**, and **4**. In this case, only the solid crystal structure of **5** could be obtained. Since **1**, **3**, and **4** show similar solid crystal structures (*S* in Figure 6), and similar dynamic behavior in solution, thus now the similar behavior in solution for **2** and **5** would support the proposal of a similar geometry for them (*A* in Figure 6). For complexes **2** and **5**, both heterocycles are equivalent both at room and at low temperatures (see Experimental). Therefore it is

evident that their *A* geometry does not account for this dynamic behavior, as in this geometry the nitrogen donor ligands are inequivalent. We should then assume that we detect a symmetric average spectrum in solution, corresponding to a fast dynamic process, which is fast enough both at room and at low temperatures. In this case, this behavior may be justified considering the dmpzH ligand which shares the triangular face with both iodido ligands (face below in isomer *A* in Figure 6). Any scrambling and/or migration of this ligand from one side to the other of the plane containing the metal, the carbonyl in the capped position, and the dmpzH in the triangular capped face (which is a symmetry plane in the *S* isomer) would explain this observation.

Complex **2** also displays a second process in solution, since in this case the  $^1\text{H}$  and  $^{13}\text{C}$  NMR spectra, both at room and at low temperatures, indicate that both methyl groups at the 3 and 5 positions of pyrazole are equivalent (see Experimental). This is a well known process, which may be explained by (a) decoordination of the pyrazole and further coordination after tautomeric equilibrium of free pyrazole, and/or by (b) deprotonation followed by intramolecular metallotropic exchange of the coordinated pyrazole [5d,15]. Therefore, this process is fast even at low temperature for **2**.

Somehow surprisingly, the  $^1\text{H}$  NMR spectrum at low temperature of the tungsten compound **5** shows the inequivalence of the hydrogen atoms of the NH groups, but at this moment we can not provide any immediate explanation for this fact, which is not detected in the similar molybdenum complex **2**.

The behavior in solution of the tungsten complex **6** is similar to that of **2** and **5**, where both indazoles are equivalent at room and at low temperatures. In this case, also the hydrogen atoms of the NH groups are inequivalent at low temperature, as occurred for **5**. The geometry of complexes **2** and **5** in the solid state was *A* (Figure 6), and therefore this geometry is associated to this dynamic behavior. As described above, both isomers, *S* and *A*, are found in the crystal structure of compound **6**. Therefore we should assume that isomer *A* is the major one in the solutions of the tungsten complex **6**, as opposite to what was observed for the molybdenum indazole complex **3**, where the major isomer in solution was *S* (see above).

No exchange between *S* and *A* geometries is detected in the solutions of any of the complexes herein described. Only one isomer is detected in the solutions of the pzH and dmpzH complexes **1**, **2**, **4**, and **5**. Both isomers are detected in the solutions of the indzH complexes **3** and **6**, but no evidences of any exchange process between them has

been found [16]. This points to a relatively high activation energy between geometries *S* and *A*, even though the differences of energies between them are small (Table 1).

### 3. Conclusions

The azole ligands are always coordinated pseudo-*cis* in the two different crystal structures found for the capped octahedron heptacoordinated  $[\text{Ml}_2(\text{CO})_3(\text{pz}^*\text{H})_2]$  complexes ( $\text{M} = \text{Mo}, \text{W}$ ;  $\text{pz}^*\text{H} = \text{pzH}, \text{dmpzH}, \text{indzH}$ ), although the iodido ligands can be coordinated either pseudo-*trans* or pseudo-*cis*. The energies between geometries *S* (those with the coordinated iodine pseudo-*trans* contain a symmetry plane) and *A* (asymmetric, as they do not present any symmetry elements) have been calculated and are really small (between  $-2.9$  and  $1.0$  Kcal/mol), but agree with what is found in the crystal structure for all the complexes, except for  $[\text{Wl}_2(\text{CO})_3(\text{indzH})_2]$ , where both isomers are found in the crystal structure. The complexes with *S* geometry undergo a dynamic process in solution which makes both heterocycles equivalent at room temperature, and unequivalent at low temperature. The behavior in solution of the other three complexes is different, as they show the equivalence of both heterocycles both at room and at low temperatures. Both isomers are found in the solutions of the indzH complexes.

### 4. Experimental

#### 4.1. General Remarks

All manipulations were performed under  $\text{N}_2$  atmosphere following conventional Schlenk techniques. Solvents were purified according to standard procedures [17].  $[\text{Ml}_2(\text{CO})_3(\text{NCMe})_2]$  ( $\text{M} = \text{Mo}, \text{W}$ ) were obtained as previously described [18]. All other reagents were obtained from the usual commercial suppliers, and used as received. Infrared spectra were recorded in a Perkin-Elmer FT-IR spectrum BX apparatus using  $0.2$  mm  $\text{CaF}_2$  cells for solutions or KBr pellets for solid samples. NMR spectra were recorded in Bruker AC-300, ARX-300, or Bruker AV-400 instruments, and the chemical shifts are referred to the internal residual solvent peak both for  $^1\text{H}$  and  $^{13}\text{C}\{^1\text{H}\}$  NMR. Assignment of the  $^{13}\text{C}\{^1\text{H}\}$  NMR data was supported by HMBC

heteronuclear experiments. Elemental analyses were performed on a Perkin-Elmer 2400B microanalyzer.

#### 4.2. $[MoI_2(CO)_3(pzH)_2]$ , **1**

$[MoI_2(CO)_3(NCMe)_2]$  (0.258 g, 0.5 mmol) was added to a solution of pzH (0.068 g, 1 mmol) in  $CH_2Cl_2$  (20 mL) at 0°C. The solution was stirred for 5 min, hexane (20 mL) was added, and the solution was concentrated at 0°C, until dark red crystals begin to precipitate. Cooling at -20 °C, afforded a dark red microcrystalline solid, which was decanted, washed with hexane (3 × 3 mL approximately), and dried in vacuo, yielding 0.246 g (86%). IR ( $CH_2Cl_2$ ,  $cm^{-1}$ ): 2030 vs, 1956 vs br, 1936 s sh. IR (KBr,  $cm^{-1}$ ): 3330 m, 3284 m, 3116 w, 2022 vs, 1941 vs, 1921 vs, 1636 w, 1519 w, 1477 w, 1406 w, 1352 w, 1266 w, 1126 m, 1060 w, 1048 m, 766 s, 674 w, 604 w, 479 w, 537 w, 468 w.  $^1H$  NMR ( $CDCl_3$ , 293 K, 300 MHz): 6.46 (d,  $J = 2.0$  Hz,  $H^4$  pzH, 2 H), 7.65 (s,  $H^{5,3}$  pzH, 2 H), 8.42 (br,  $H^{3,5}$  pzH, 2 H), 11.13 (br, NH, 2 H).  $^1H$  NMR ( $Me_2CO-d_6$ , 193 K, 400 MHz): 6.63 (s,  $H^4$  pzH, 1 H), 6.74 (s,  $H^4$  pzH, 1 H), 7.06 (s, NH, 1 H), 8.02 (s,  $H^{5,3}$  pzH, 1 H), 8.21 (s,  $H^{5,3}$  pzH, 1 H), 8.40 (s,  $H^{3,5}$  pzH, 1 H), 8.64 (s,  $H^{3,5}$  pzH, 1 H), 12.70 (s, NH, 1 H).  $^{13}C\{^1H\}$  NMR ( $CDCl_3$ , 293 K, 75.78 MHz): 107.6 (s,  $C^4H$  pzH), 131.8 (s,  $C^{3,5}H$  pzH), 146.3 (s,  $C^{5,3}H$  pzH), 229.7 (s, CO).  $^{13}C\{^1H\}$  NMR ( $Me_2CO-d_6$ , 193 K, 100.5 MHz): 105.8 (s, 1  $C^4H$  pzH), 106.7 (s, 1  $C^4H$  pzH), 128.4 (s, 1  $C^{3,5}H$  pzH), 132.4 (s, 1  $C^{3,5}H$  pzH), 136.5 (s, 1  $C^{5,3}H$  pzH), 145.7 (s, 1  $C^{5,3}H$  pzH), CO not detected. Anal. Calcd. for  $C_9H_8MoI_2N_4O_3$ : C, 18.97; H, 1.41; N, 9.83. Found: C, 19.23; H, 1.33; N, 9.58%.

#### 4.3. $[MoI_2(CO)_3(dmpzH)_2]$ , **2**

$[MoI_2(CO)_3(NCMe)_2]$  (0.104 g, 0.2 mmol) was added to a solution of dmpzH (0.039 g, 0.4 mmol) in  $CH_2Cl_2$  (10 mL) at 0°C. The solution was stirred for 5 min and the solvent was removed at 0°C. The red brown residue was extracted with  $Et_2O$  (10 mL), hexane (20 mL) was added, and the solution was concentrated until red brown crystals begin to precipitate. Cooling at -20 °C, afforded a red brown microcrystalline solid, which was decanted, washed with hexane (3 × 3 mL approximately), and dried in vacuo, yielding 0.112 g (89%). IR ( $CH_2Cl_2$ ,  $cm^{-1}$ ): 2030 vs, 1968 s, 1926 s. IR (KBr,  $cm^{-1}$ ): 3392 m, 3331 m, 2927 w, 2017 vs 1955 vs, 1944 s, 1914 vs, 1569 m, 1560 m, 1541 m, 1508 m, 1418 w, 1277 m, 1170 m, 1152 m, 1035 m, 1020 m, 821 w, 802 m, 650 m, 550 m, 526

m, 478 m.  $^1\text{H}$  NMR ( $\text{CDCl}_3$ , 293 K, 300 MHz): 2.36 (s,  $\text{CH}_3$  dmpzH, 12 H), 5.97 (s,  $H^4$  dmpzH, 2 H), 10.79 (br, NH, 2 H).  $^1\text{H}$  NMR ( $\text{Me}_2\text{CO}-d_6$ , 193 K, 400 MHz): 2.35 (s,  $\text{CH}_3$  dmpzH, 12 H), 6.27 (s,  $H^4$  dmpzH, 2 H), 11.30 (br, NH, 2 H).  $^{13}\text{C}\{^1\text{H}\}$  NMR ( $\text{CDCl}_3$ , 293 K, 75,78 MHz): 11.8 (s,  $\text{CH}_3$  dmpzH), 144.8 (s,  $\text{C}^3$  and  $\text{C}^5$  dmpzH), 106.0 (s,  $\text{C}^4\text{H}$  dmpzH), CO not observed.  $^{13}\text{C}\{^1\text{H}\}$  NMR ( $\text{Me}_2\text{CO}-d_6$ , 193 K, 100.5 MHz): 11.0 (s,  $\text{CH}_3$  dmpzH), 105.8 (s,  $\text{C}^4\text{H}$  dmpzH), 145.0 (s,  $\text{C}^3$  and  $\text{C}^5$  dmpzH), CO not observed. Anal. Calcd. for  $\text{C}_{13}\text{H}_{16}\text{MoI}_2\text{N}_4\text{O}_3$ : C, 24.94; H, 2.58; N, 8.95. Found: C, 24.76; H, 2.63; N, 9.03%.

#### 4.4. $[\text{MoI}_2(\text{CO})_3(\text{indzH})_2]$ , **3**

$[\text{MoI}_2(\text{CO})_3(\text{NCMe})_2]$  (0.103 g, 0.2 mmol) was added to a solution of indzH (0.048 g, 0.4 mmol) in  $\text{CH}_2\text{Cl}_2$  (10 mL) at  $0^\circ\text{C}$ . The solution was stirred for 5 min. Work up as for **1** yielded 0.114 g (85%), as a orange crystalline solid. IR ( $\text{CH}_2\text{Cl}_2$ ,  $\text{cm}^{-1}$ ): 2031 s, 1958 s, 1942 s. IR (KBr,  $\text{cm}^{-1}$ ): 3330 s, 2022 vs, 1938 vs, 1925 vs, 1627 s, 1584 w, 1512 m, 1473 m, 1434 w, 1358 s, 1325 w, 1270 m, 1244 m, 1213 w, 1150 w, 1126 m, 1078 s, 1001 m, 959 s, 895 w, 861 m, 840 w, 778 w, 748 s, 645 s, 605 w, 538 w, 486 m, 464 m, 444 w, 421 s.  $^1\text{H}$  NMR ( $\text{Me}_2\text{CO}-d_6$ , 293 K, 400 MHz): 7.27 (t,  $J = 7.0$  Hz,  $H^5$  indzH *m* isomer, 2 H), 7.34 (t,  $J = 7.2$  Hz,  $H^5$  indzH *M* isomer, 2 H), 7.50 (t,  $J = 8.2$  Hz,  $H^6$  indzH *m* isomer, 2 H), 7.56 (t,  $J = 7.0$  Hz,  $H^6$  indzH *M* isomer, 2 H), 7.68 (d,  $J = 8.4$  Hz,  $H^7$  indzH *M* isomer, 2 H), 7.70 (d,  $J = 10.6$  Hz,  $H^7$  indzH *m* isomer, 2 H), 7.90 (d,  $J = 9.2$  Hz,  $H^4$  indzH *m* isomer, 2 H), 7.97 (d,  $J = 9.2$  Hz,  $H^4$  indzH *M* isomer, 2 H), 8.42 (s,  $H^3$  indzH *m* isomer, 2 H), 8.87 (s,  $H^3$  indzH *M* isomer, 2 H), 12.67 (s, NH indzH *M* isomer, 2 H), 12.90 (s, NH indzH *m* isomer, 2 H). *M/m* ratio = 90/10.  $^1\text{H}$  NMR (recently prepared solution from frozen  $\text{Me}_2\text{CO}-d_6$ , 193 K, 400 MHz): 7.23 (t,  $J = 7$  Hz,  $H^5$  indzH, 1 H), 7.35 (t,  $J = 7$  Hz,  $H^5$  indzH, 1 H), 7.49 (t,  $J = 7$  Hz,  $H^6$  indzH, 1 H), 7.60 (t,  $J = 7$  Hz,  $H^6$  indzH, 1 H), 7.70 (d,  $J = 8$  Hz,  $H^7$  indzH, 1 H), 7.72 (d,  $J = 8$  Hz,  $H^7$  indzH, 1 H), 7.92 (s,  $H^3$  indzH, 1 H), 8.01 (d,  $J = 9$  Hz,  $H^4$  indzH, 1 H), 8.06 (d,  $J = 9$  Hz,  $H^4$  indzH, 1 H), 8.91 (s,  $H^3$  indzH, 1 H), 9.39 (s, NH indzH, 1 H), 12.85 (s, NH indzH, 1 H), all the signals from the *M* isomer.  $^{13}\text{C}\{^1\text{H}\}$  NMR ( $\text{Me}_2\text{CO}-d_6$ , 293 K, 100.5 MHz): 112.6 (s,  $\text{C}^7$  indzH), 123.1 (s,  $\text{C}^4$  indzH), 124.3 (s,  $\text{C}^5$  indzH), 124.7 (s,  $\text{C}^{3a}$  indzH), 131.3 (s,  $\text{C}^6$  indzH), 143.4 (s,  $\text{C}^{7a}$  indzH), 144.0 (s,  $\text{C}^3$  indzH), 232.3 (s, CO), all the signals from the *M* isomer.  $^{13}\text{C}\{^1\text{H}\}$  NMR ( $\text{Me}_2\text{CO}-d_6$ , 193 K, 100.5 MHz): 109.9 (s, 1  $\text{C}^7$  indzH), 110.1 (s, 1  $\text{C}^7$  indzH), 120.7 (s, 1  $\text{C}^4$  indzH), 121.2 (s, 1  $\text{C}^4$  indzH), 122.1 (s,

2  $C^5$  indzH), 129.0 (s, 2  $C^6$  indzH), 140.3 (s, 1  $C^3$  indzH), 141.7 (s, 1  $C^3$  indzH), all the signals from the *M* isomer,  $C^{3a}$  indzH,  $C^{7a}$  indzH, and CO not observed. Anal. Calcd. for  $C_{17}H_{12}MoI_2N_4O_3$ : C, 30.47; H, 1.80; N, 8.36. Found: C, 30.53; H, 1.75; N, 8.12.

#### 4.5. $[WI_2(CO)_3(pzH)_2]$ , **4**

$[WI_2(CO)_3(NCMe)_2]$  (0.302 g, 0.5 mmol) was added to a solution of pzH (0.69 g, 1.0 mmol) in  $CH_2Cl_2$  (10 mL) at 0°C. The solution was stirred for 5 min. Work up as for **1** yielded 0.263 g (80%), as a orange crystalline solid. IR ( $CH_2Cl_2$ ,  $cm^{-1}$ ): 2022 vs, 1938 vs. IR (KBr,  $cm^{-1}$ ): 3448 s, 3275 s, 2012 s, 1902 vs, 1654 m, 1637 m, 1477 m, 1406 m, 1350 w, 1266 w, 1125 s, 1060 m, 1048 s, 907 w, 766 s, 670 m, 578 m, 544 m.  $^1H$  NMR ( $CDCl_3$ , 293 K, 300 MHz): 6.46 (s,  $H^4$  pzH, 2 H), 7.65 (s,  $H^{3,5}$  pzH, 2 H), 8.36 (s,  $H^{5,4}$  pzH, 2 H), 11.28 (br s, NH, 2 H).  $^1H$  NMR ( $Me_2CO-d_6$ , 193 K, 400 MHz): 6.59 (s,  $H^4$  pzH, 2 H), 7.00 (s,  $H^{3,5}$  pzH, 1 H), 7.0 (br s, NH, 1 H), 7.98 (s,  $H^{5,3}$  pzH, 1 H), 8.25 (s,  $H^{3,5}$  pzH, 1 H), 8.57 (s,  $H^{5,3}$  pzH, 1 H), 12.2 (br s, NH, 1 H).  $^{13}C\{^1H\}$  NMR ( $CDCl_3$ , 293 K, 75,78 MHz): 108.2 (s,  $C^4H$  pzH), 132.0 (s,  $C^{5,3}H$  pzH), 146.7 (s,  $C^{3,5}H$  pzH), 223.3 (s, CO).  $^{13}C\{^1H\}$  NMR ( $Me_2CO-d_6$ , 193 K, 100.5 MHz): 87.9 (s, 1  $C^4H$  pzH), 105.7 (s, 1  $C^4H$  pzH), 107.9 (s, 1  $C^{3,5}H$  pzH), 128.4 (s, 1  $C^{3,5}H$  pzH), 134.1 (s, 1  $C^{5,3}H$  pzH), 136.5 (s, 1  $C^{5,3}H$  pzH), CO not observed. Anal. Calcd. for  $C_9H_8WI_2N_4O_3$ : C, 16.43; H, 1.23; N, 8.51. Found: C, 16.70; H, 1.21; N, 8.43.

#### 4.6. $[WI_2(CO)_3(dmpzH)_2]$ , **5**

$[WI_2(CO)_3(NCMe)_2]$  (0.302 g, 0.5 mmol) was added to a solution of dmpzH (0.096 g, 1.0 mmol) in  $CH_2Cl_2$  (10 mL) at 0°C. The solution was stirred for 5 min and the solvent was removed at 0°C. Work up as for **2** yielded 0.292 g (82%), as a yellow-orange crystalline solid. IR ( $CH_2Cl_2$ ,  $cm^{-1}$ ): 2024 vs, 1950 vs br. IR (KBr,  $cm^{-1}$ ): 3385 m, 3329 m, 2010 vs, 1928 vs, 1890 vs, 1569 m, 1508 w, 1420 w, 1366 w, 1277 m, 1169 w, 1150 w, 1038 m, 1020 m, 819 w, 803 w, 649 d, 588 w, 524 w.  $^1H$  NMR ( $CDCl_3$ , 293 K, 300 MHz): 2.25 (s,  $CH_3$  dmpzH, 6 H), 2.33 (s,  $CH_3$  dmpzH, 6 H), 5.94 (s,  $H^4$  dmpzH, 2 H), 11.07 (br, NH, 2 H).  $^1H$  NMR ( $Me_2CO-d_6$ , 193 K, 400 MHz): 2.27 (s,  $CH_3$  dmpzH, 12 H), 6.12 (s,  $H^4$  dmpzH, 2 H), 7.21 (s, NH, 1 H), 7.69 (s, NH, 1 H).  $^{13}C\{^1H\}$  NMR ( $CDCl_3$ , 293 K, 75,78 MHz): 11.0 ( $CH_3$  dmpzH), 16.0 ( $CH_3$  dmpzH), 108.4 (s,  $C^4H$  dmpzH), 143.1 (s,  $C^{5,3}$  dmpzH), 155.4 (s,  $C^{3,5}$  dmpzH), 222.8 (s, CO).  $^{13}C\{^1H\}$  NMR ( $Me_2CO-d_6$ , 193 K, 100.5 MHz): 10.2 ( $CH_3$  dmpzH), 104.8 (s,  $C^4H$  dmpzH), 144.2 (s,

$C^5$  and  $C^3$  dmpzH), 201.3 (s, CO). Anal. Calcd. for  $C_{13}H_{16}Wl_2N_4O_3$ : C, 21.87; H, 2.26; N, 7.85. Found: C, 22.06; H, 2.01; N, 7.63%.

#### 4.7. $[Wl_2(CO)_3(indzH)_2]$ , **6**

$[Wl_2(CO)_3(NCMe)_2]$  (0.121 g, 0.2 mmol) was added to a solution of indzH (0.048 g, 0.4 mmol) in  $CH_2Cl_2$  (10 mL) at  $0^\circ C$ . The solution was stirred for 5 min. Work up as for **1** yielded 0.131 g (86%), as an orange crystalline solid. IR ( $CH_2Cl_2$ ,  $cm^{-1}$ ): 2023 vs, 1940 s, 1922 s. IR (KBr,  $cm^{-1}$ ): 3322 s, 2008 vs, 1925 vs, 1910 vs, 1628 s, 1509 m, 1470 w, 1435 w, 1358 s, 1268 w, 1244 m, 1150 w, 1125 w, 1076 m, 1000 w, 960 m, 860 w, 838 w, 749 s, 645 s, 615 w, 542 w, 485 m, 427 w.  $^1H$  NMR ( $Me_2CO-d_6$ , 293 K, 400 MHz): 7.19 (t,  $J = 7.5$  Hz,  $H^6$  indzH *m* isomer, 2 H), 7.34 (t,  $J = 7.2$  Hz,  $H^6$  indzH *M* isomer, 2 H), 7.41 (t,  $J = 7.2$  Hz,  $H^5$  indzH *m* isomer, 2 H), 7.60 (t,  $J = 7.0$  Hz,  $H^5$  indzH *M* isomer, 2 H), 7.66 (d,  $J = 7.9$  Hz,  $H^4$  indzH *m* isomer, 2 H), 7.68 (d,  $J = 8.8$  Hz,  $H^4$  indzH *M* isomer, 2 H), 7.83 (d,  $J = 6.4$  Hz,  $H^7$  indzH *m* isomer, 2 H), 8.02 (d,  $J = 10.4$  Hz,  $H^7$  indzH *M* isomer, 2 H), 8.56 (s,  $H^3$  indzH *m* isomer, 2 H), 8.97 (s,  $H^3$  indzH *M* isomer, 2 H), 12.68 (s, NH indzH *M* isomer, 2 H), 12.90 (s, NH indzH *m* isomer, 2 H). *M/m* ratio = 90/10.  $^1H$  NMR [recently prepared solution from frozen  $Me_2CO-d_6$ , 193 K, 400 MHz]: 7.21 (t,  $J = 7$  Hz,  $H^5$  indzH, 2 H), 7.48 (t,  $J = 7$  Hz,  $H^6$  indzH, 2 H), 7.68 (d,  $J = 10$  Hz,  $H^7$  indzH, 2 H), 7.90 (d,  $J = 8$  Hz,  $H^4$  indzH, 2 H), 7.91 (s, NH indzH, 1 H), 8.33 (s,  $H^3$  indzH, 2 H), 9.38 (s, NH indzH, 1 H), all the signals from the *M* isomer.  $^{13}C$  { $^1H$ } NMR ( $Me_2CO-d_6$ , 293 K, 100.5 MHz): 112.6 (s,  $C^7$  indzH), 123.2 (s,  $C^4$  indzH), 124.5 (s,  $C^5$  indzH), 124.7 (s,  $C^{3a}$  indzH), 131.6 (s,  $C^6$  indzH), 143.5 (s,  $C^{7a}$  indzH), 144.8 (s,  $C^3$  indzH), 226.0 (s, CO), all the signals from the *M* isomer.  $^{13}C$  { $^1H$ } NMR ( $Me_2CO-d_6$ , 193 K, 100.5 MHz): 109.7.5 (s,  $C^7$  indzH), 120.6 (s,  $C^4$  indzH), 121.9 (s,  $C^5$  indzH), 132.7 (s, 1  $C^6$  indzH), 139.0 (s, 1  $C^3$  indzH), all the signals from the *M* isomer,  $C^{3a}$  indzH,  $C^{7a}$  indzH, and CO not observed. Anal. Calcd. for  $C_{17}H_{12}Wl_2N_4O_3$ : C, 26.94; H, 1.60; N, 7.39. Found: C, 26.95; H, 1.63; N, 7.29.

#### 4.8. Crystal structure determination for compounds **1**, **3**, **4**, **5**, and **6**

Crystals were grown by slow diffusion of hexane into concentrated solutions of the complexes in  $CH_2Cl_2$  at  $-20^\circ C$ . Relevant crystallographic details can be found in the CIF. For **1**, **4**, and **5**, a crystal was attached to a glass fiber and transferred to a Bruker AXS SMART 1000 diffractometer with graphite monochromatized Mo  $K_\alpha$  X-radiation

and a CCD area detector. Raw frame data were integrated with the SAINT program [19], and a semi-empirical absorption correction was applied with the program SADABS [20]. For **3** and **6**, their crystal structure determinations were accomplished on an Oxford Diffraction Xcalibur S diffractometer, using the CrysAlis program [21], for data collection, cell refinement, data reduction, and multiscan absorption correction. The crystal structure determinations were effected at  $-100\text{ }^{\circ}\text{C}$  (Mo  $K\alpha$  radiation,  $\alpha = 0.71073\text{ \AA}$ ). All the structures were solved by direct methods with SHELXTL [22]. All non-hydrogen atoms were refined anisotropically. Hydrogen atoms were set in calculated positions and refined as riding atoms, with a common thermal parameter. All calculations and graphics were made with Olex2 [23]. Distances and angles of hydrogen bonds were calculated with PARST<sup>[24]</sup> (normalized values) [25].

CCDC 1492603 (for **1**), 1492604 (for **3**), 1492605 (for **4**), 1492606 (for **5**), and 1492607 (for **6**) contain the supplementary crystallographic data for this paper. These data can be obtained free of charge from The Cambridge Crystallographic Data Centre.

#### 4.9. Computational details

All calculations have been performed using the Gaussian 09 program package [26], in which the hybrid method B3LYP was applied with the Becke three-parameter exchange functional [27], and the Lee-Yang-Parr correlation functional [28]. Effective core potentials (ECP) and their associated double- $\zeta$  LANL2DZ basis set were used for the molybdenum, tungsten and iodide atoms [29]. The light elements (O, N, C, and H) were described with the 6-31G\*\* basis [30]. Geometry optimizations were performed under no symmetry restrictions, using initial coordinates derived from X-ray data of the same complexes, and frequency analyses were performed to ensure that a minimum structure with no imaginary frequencies was achieved in each case.

#### Acknowledgements

This research was supported by the Spanish MINECO (Project CTQ2013-41067-P).

Table 2. Crystal Data and Refinement Details for compounds **1**, **3**, **4**, **5**, and **6**.

	<b>1</b>	<b>3</b>	<b>4</b>	<b>5</b>	<b>6</b>
formula	C <sub>9</sub> H <sub>8</sub> I <sub>2</sub> MoN <sub>4</sub> O <sub>3</sub>	C <sub>17</sub> H <sub>12</sub> I <sub>2</sub> MoN <sub>4</sub> O <sub>3</sub>	C <sub>9</sub> H <sub>8</sub> I <sub>2</sub> N <sub>4</sub> O <sub>3</sub> W	C <sub>13</sub> H <sub>16</sub> I <sub>2</sub> N <sub>4</sub> O <sub>3</sub> W	C <sub>17</sub> H <sub>12</sub> I <sub>2</sub> N <sub>4</sub> O <sub>3</sub> W
fw	569.93	670.05	657.84	713.95	757.96
cryst system	Monoclinic	Monoclinic	Monoclinic	Monoclinic	Monoclinic
space group	P2(1)/n	P2(1)/n	P2(1)/n	P2(1)/n	P2(1)/c
<i>a</i> , Å	9.992(2)	18.1097(6)	9.958(4)	10.800(4)	14.9302(7)
<i>b</i> , Å	12.696(3)	12.2469(3)	12.626(5)	14.841(6)	18.2043(5)
<i>c</i> , Å	12.377(3)	9.0308(3)	12.324(5)	12.411(5)	15.0096(6)
$\alpha$ , deg	90	90	90	90	90
$\beta$ , deg	96.536(6)	93.927(3)	96.372(7)	91.552(7)	101.492(4)
$\gamma$ , deg	90	90	90	90	90
<i>V</i> , Å <sup>3</sup>	1559.9(7)	1998.22(11)	1539.9(10)	1988.6(14)	3997.7(3)
<i>Z</i>	4	4	4	4	8
<i>T</i> , K	295(2)	173(2)	296(2)	299(2)	173(2)
<i>d</i> <sub>calc</sub> , g cm <sup>-3</sup>	2.427	2.227	2.838	2.385	2.519
F(000)	1048	1256	2076	1304	2768
$\lambda$ (Mo K $\alpha$ ), Å	0.71073	0.71073	0.71073	0.71073	0.71073
crystal size, mm; color	0.21 × 0.1 × 0.09, red	0.2 × 0.2 × 0.1, yellow	0.43 × 0.3 × 0.28, red	0.36 × 0.36 × 0.25, orange	0.3 × 0.1 × 0.1, yellow
$\mu$ , mm <sup>-1</sup>	4.807	3.771	11.519	8.930	8.893
scan range, deg	2.31 to 23.29	2.01 to 27.00	2.32 to 23.27	2.33 to 23.33	2.08 to 26.00

	Semi-empirical from equivalents				
absorption correction					
corr. factors (max, min)	1.000, 0.585	0.704, 0.519	1.000, 0.586	1.000, 0.536	1.000, 0.229
no of refl measured	6865	38664	6755	8391	22940
no of ref independent [R(int)]	2247 [0.0256]	4358 [0.0653]	2196 [0.0387]	2872 [0.0272]	7544 [0.0595]
GOF on F <sup>2</sup>	1.051	1.037	1.154	1.141	0.980
no. of parameters	172	244	173	213	487
residuals R, wR2	0.0211, 0.0545	0.0442, 0.1132	0.0299, 0.0794	0.0270, 0.0655	0.0375, 0.0933

---

**References**

- [1] (a) D. Braga, *J. Chem. Soc., Dalton Trans.* (2000) 3705-3713;  
(b) G. R. Desiraju, *J. Chem. Soc., Dalton Trans.* (2000) 3745-3751.
- [2] (a) S. R. Stobart, K. R. Dixon, D. T. Eadie, J. L. Atwood, M. D. Zaworotko, *Angew. Chem. Int. Ed. Engl.* 19 (1980) 931-932.  
(b) P. Paredes, D. Miguel, F. Villafaña, *Eur. J. Inorg. Chem.* (2003) 995-1004.
- [3] Some leading reviews: (a) P. Buchwalter, J. Rosé, P. Braunstein, *Chem. Rev.* 115 (2015) 28–126;  
(b) R. J. Eisenhart, L. J. Clouston, C. C. Lu, *Acc. Chem. Res.* 48 (2015) 2885–2894;  
(c) S. Matsunaga, M. Shibasaki, *Chem. Commun.* 50 (2014) 1044-1057;  
(d) I. Bratko, M. Gómez, *Dalton Trans.* 42 (2013) 10664–10681;  
(e) B. G. Cooper, J. W. Napoline, C. M. Thomas, *Catal. Rev. Sci. Eng.* 54 (2012) 1-40;  
(f) V. Ritleng, M. J. Chetcuti, *Chem. Rev.* 107 (2007) 797-858;  
(g) A. Ceccon, S. Santi, L. Orian, A. Bisello, *Coord. Chem. Rev.* 248 (2004) 683–724;  
(h) J. P. Collman, R. Boulatov, *Angew. Chem. Int. Ed.* 41 (2002) 3948-3961;  
(i) L. H. Gade, *Angew. Chem. Int. Ed.* 39 (2000) 2658-2678;  
(j) N. Wheatley, P. Kalck, *Chem. Rev.* 99 (1999) 3379-3419.
- [4] Crystal structures reported: (a) F. A. Cotton, B. A. Frenz, A. G. Stanislawski, *Inorg. Chim. Acta* 7 (1973) 503-508;  
(b) S. J. Rettig, A. Storr, J. Trotter, *Can. J. Chem.* 66 (1988) 97-100;  
(c) F. A. Cotton, R. L. Luck, *Acta Crystallogr., Sect. C: Cryst. Struct. Commun.* 46 (1990) 138-140;  
(d) K. Sugawara, S. Hikichi, M. Akita, *J. Chem. Soc., Dalton Trans.* (2002) 4514-4524;  
(e) J. Pérez, D. Morales, S. Nieto, L. Riera, V. Riera, D. Miguel, *Dalton Trans.* (2005) 884-888;  
(f) S. Nieto, J. Pérez, L. Riera, V. Riera, D. Miguel, J. A. Golen, A. L. Rheingold, *Inorg. Chem.* 46 (2007) 3407-3418;  
(g) M. Arroyo, M. T. García-de-Prada, C. García-Martín, V. García-Pacios, R. García-Rodríguez, P. Gómez-Iglesias, F. Lorenzo, I. Martín-Moreno, D. Miguel, F. Villafaña, *J. Organomet. Chem.* 694 (2009) 3190–3199;  
(h) P. Paredes, A. López-Calzada, D. Miguel, F. Villafaña, *Dalton Trans.* 39 (2010) 10099–10104;

- (i) M. Arroyo, P. Gómez-Iglesias, J. M. Martín-Alvarez, C. M. Alvarez, D. Miguel, F. Villafane, *Inorg. Chem.* 51 (2012) 6070-6080;
- (j) S. Kumar, G. Mani, *Polyhedron* 99 (2015) 47-52.
- [5] (a) P. Paredes, M. Arroyo, D. Miguel, F. Villafañe, *J. Organomet. Chem.* 667 (2003) 120-125;
- (b) M. Arroyo, A. López-Sanvicente, D. Miguel, F. Villafañe, *Eur. J. Inorg. Chem.* (2005) 4430-4437;
- (c) M. Arroyo, D. Miguel, F. Villafañe, S. Nieto, J. Pérez, L. Riera, *Inorg. Chem.* 45 (2006) 7018-7026;
- (d) V. García-Pacios, M. Arroyo, N. Antón, D. Miguel, F. Villafañe, *Dalton Trans.* (2009) 2135-2141;
- (e) P. Gómez-Iglesias, M. Arroyo, S. Bajo, C. Strohmman, D. Miguel, F. Villafañe, *Inorg. Chem.* 53 (2014) 12437-12448.
- [6] F. Villafañe. *Coord. Chem. Rev.* 281 (2014) 86-99, and references therein.
- [7] P. K. Baker, M. van Kampen, C. Roos, J. Spaeth, *Trans. Met. Chem.* 19 (1994) 165-168.
- [8] The terms pseudo-*trans* or pseudo-*cis* are referred to the ideal *trans* or *cis* positions of a related uncapped octahedron. The pseudo-*trans* angles range from *ca.* 155° to 165°, whereas those pseudo-*cis* display values between *ca.* 73° and 115°.
- [9] (a) M. G. B. Drew, P. K. Baker, E. M. Armstrong, S. G. Fraser, *Polyhedron* 7 (1988) 245-247;
- (b) M. G. B. Drew, P. K. Baker, E. M. Armstrong, S. G. Fraser, D. J. Muldoon, A. J. Lavery, A. Shawcross, *Polyhedron* 14 (1995) 617-620;
- (c) P. K. Baker, D. J. Muldoon, M. B. Hursthouse, S. J. Coles, A. J. Lavery, A. Shawcross, *Z. Naturforsch., B: Chem. Sci.* 51b (1996) 263-266;
- (d) P. K. Baker, M. G. B. Drew, M. M. Meehan, E. E. Parker, A. E. Underhill, *J. Organomet. Chem.* 560 (1998) 191-196;
- (e) P.K. Baker, M. M. Meehan, M. G. B. Drew, *Transition Met. Chem.* 24 (1999) 333-336;
- (f) P. K. Baker, E. Samson, P. L. Veale, M. G.B. Drew, *Polyhedron* 19 (2000) 147-153.
- [10] (a) P. K. Baker, M. B. Hursthouse, A. I. Karaulov, A. J. Lavery, K. M. A. Malik, D. J. Muldoon, A. Shawcross, *J. Chem. Soc., Dalton Trans.* (1994) 3493-3498;
- (b) P. K. Baker, M. E. Harman, M. B. Hursthouse, A. I. Karaulov, A. J. Lavery, K. M. A. Malik, D. J. Muldoon, A. Shawcross, *J. Organomet. Chem.* 494 (1995) 205-213;

- (c) P. K. Baker, S. J. Coles, M. C. Durrant, S. D. Harris, D. L. Hughes, M. B. Hursthouse, R. L. Richards, *J. Chem. Soc., Dalton Trans.* (1996) 4003-4010;
- (d) R. Sommer, P. Lönnecke, J. Reinhold, P. K. Baker, E. Hey-Hawkins, *Organometallics* 24 (2005) 5256-5266.
- [11] (a) M. G. B. Drew, J. D. Wilkins, *J. Chem. Soc., Dalton Trans.* (1977) 194-197;
- (b) P. K. Baker, M. B. Hursthouse, L. A. Latif, K. M. A. Malik. *J. Chem. Crystall.* 28 (1998) 639-643;
- (c) P. K. Baker, S. J. Coles, N. S. Harrison, L. A. Latif, M. M. Meehan, M. B. Hursthouse, *J. Organomet. Chem.* 566 (1998) 245-250;
- (d) P. K. Baker, A. I. Clark, M. M. Meehan, E. E. Parker, A. E. Underhill, M. G. B. Drew, M. C. Durrant, R. L. Richards, *Transition Met. Chem.* 23 (1998) 155-157;
- (e) P. K. Baker, L. A. Latif, M. M. Meehan, S. Zanin, M. G. B. Drew, *Polyhedron* 18 (1999) 257-261;
- (f) R. Sommer, P. Lönnecke, P. K. Baker, E. Hey-Hawkins, *Inorg. Chem. Commun.* 5 (2002) 115-118.
- [12] (a) G. A. Jeffrey, *An Introduction to Hydrogen Bonding*, Oxford University Press, New York, 1997, ch. 2;
- (b) T. Steiner, *Angew. Chem., Int. Ed.* 41 (2002) 48-76.
- [13] R. Contreras, M. Valderrama, E. M. Orellana, D. Boys, D. Carmona, L. A. Oro, M. P. Lamata, J. Ferrer, *J. Organomet. Chem.* 606 (2000) 197-202.
- [14] T. Beringhelli, G. D'Alfonso, M. Panigati, F. Porta, P. Mercandelli, M. Moret, A. Sironi, *Organometallics* 17 (1998) 3282-3292.
- [15] (a) G.W. Bushnell, K. R. Dixon, D. Eadie, S. R. Stobart, *Inorg. Chem.* 20 (1981) 1545-1552;
- (b) J. Cámpora, J. A. López, C. M. Maya, P. Palma, E. Carmona, C. Ruiz, *Organometallics* 19 (2000) 2707-2715.
- [16] EXSY experiments were carried out on **3** and **6** with mixing times from 100 to 800 ms, and no evidences of exchange between signals of the **S** and **A** isomers could be detected.
- [17] D. D. Perrin, W. L. F. Armarego, *Purification of Laboratory Chemicals*; 3rd ed.; Pergamon Press: Oxford, 1988.
- [18] P. K. Baker, S. G. Fraser, E. M. Keys, *J. Organomet. Chem.* 309 (1986) 319-321.
- [19] SAINT+. *SAX area detector integration program*. Version 6.02. Bruker AXS, Inc. Madison, WI, 1999.

- [20] G. M. Sheldrick, *SADABS, Empirical Absorption Correction Program*. University of Göttingen: Göttingen, Germany, 1997.
- [21] *Oxford Diffraction, CrysAlis CCD and CrysAlis RED*. Oxford Diffraction Ltd, Yarnton, England, 2008.
- [22] (a) G. M. Sheldrick, *SHELXTL, An integrated system for solving, refining, and displaying crystal structures from diffraction data*. Version 5.1. Bruker AXS, Inc. Madison, WI, 1998;
- (b) G. M. Sheldrick, *Acta Cryst.* A64 (2008) 112-122.
- [23] O. V. Dolomanov, L. J. Bourhis, R. J. Gildea, J. A. K. Howard, H. Puschmann, *J. Appl. Cryst.* 42 (2009) 339-341.
- [24] (a) M. Nardelli, *Computer and Chemistry* 7 (1983) 95-98;
- (b) M. Nardelli, *J. Appl. Cryst.* 28 (1995) 659.
- [25] (a) G. A. Jeffrey, L. Lewis, *Carbohydr. Res.* 60 (1978) 179-182;
- (b) R. Taylor, O. Kennard, *Acta Cryst.* B39 (1983) 133-138.
- [26] *Gaussian 09*, Revision A.02, M. J. Frisch, G. W. Trucks, H. B. Schlegel, G. E. Scuseria, M. A. Robb, J. R. Cheeseman, G. Scalmani, V. Barone, B. Mennucci, G. A. Petersson, H. Nakatsuji, M. Caricato, X. Li, H. P. Hratchian, A. F. Izmaylov, J. Bloino, G. Zheng, J. L. Sonnenberg, M. Hada, M. Ehara, K. Toyota, R. Fukuda, J. Hasegawa, M. Ishida, T. Nakajima, Y. Honda, O. Kitao, H. Nakai, T. Vreven, J. A. Montgomery Jr., J. E. Peralta, F. Ogliaro, M. Bearpark, J. J. Heyd, E. Brothers, K. N. Kudin, V. N. Staroverov, R. Kobayashi, J. Normand, K. Raghavachari, A. Rendell, J. C. Burant, S. S. Iyengar, J. Tomasi, M. Cossi, N. Rega, J. M. Millam, M. Klene, J. E. Knox, J. B. Cross, V. Bakken, C. Adamo, J. Jaramillo, R. Gomperts, R. E. Stratmann, O. Yazyev, A. J. Austin, R. Cammi, C. Pomelli, J. W. Ochterski, R. L. Martin, K. Morokuma, V. G. Zakrzewski, G. A. Voth, P. Salvador, J. J. Dannenberg, S. Dapprich, A. D. Daniels, O. Farkas, J. B. Foresman, J. V. Ortiz, J. Cioslowski and D. J. Fox, Gaussian, Inc., Wallingford CT, 2009.
- [27] A. D. Becke, *J. Chem. Phys.* 98 (1993) 5648-5652.
- [28] C. Lee, W. Yang, R. G. Parr, *Phys. Rev. B* 37 (1988) 785-789.
- [29] P. J. Hay, W. R. Wadt, *J. Chem. Phys.* 82 (1985) 299-310.
- [30] (a) P. C. Hariharan, J. A. Pople, *Theor. Chim. Acta* 28 (1973) 213-222;
- (b) G. A. Petersson, M. A. Al-Laham, *J. Chem. Phys.* 94 (1991) 6081-6090;
- (c) G. A. Petersson, A. Bennett, T. G. Tensfeldt, M. A. Al-Laham, W. A.; Shirley, J. Mantzaris, *J. Chem. Phys.* 89 (1988) 2193-2218.

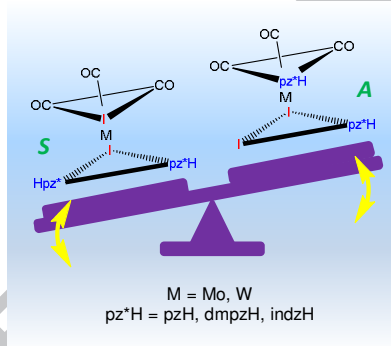
## Synopsis and Pictogram for Preliminary Contents

**Syntheses, solid structures, and behavior in solution of  $[Ml_2(CO)_3(\text{pyrazole})_2]$  complexes (M = Mo, W)**

Paloma Paredes,<sup>a</sup> Fernando Lorenzo,<sup>a</sup> Sonia Bajo,<sup>a</sup> Elena Cuéllar,<sup>a</sup> Carsten Strohmann,<sup>b</sup>  
 Jose M. Martín-Alvarez,<sup>a</sup> Daniel Miguel,<sup>a</sup> and Fernando Villafañe\*<sup>a</sup>

<sup>a</sup> *GIR MIOMeT-IU Cinquima-Química Inorgánica, Facultad de Ciencias, Campus Miguel Delibes, Universidad de Valladolid, 47011 Valladolid, Spain.*

<sup>b</sup> *Anorganische Chemie, Technische Universität Dortmund, Otto-Hahn-Straße 6, 44227 Dortmund, Germany.*



Molybdenum and tungsten heptacoordinated complexes  $[Ml_2(CO)_3(\text{pyrazole})_2]$  have been synthesized and characterized. In solid state they present two possible geometries, either *S* (symmetric) or *A* (asymmetric), with very similar calculated energies. All the complexes are fluxional, each isomer showing a different behavior in solution.

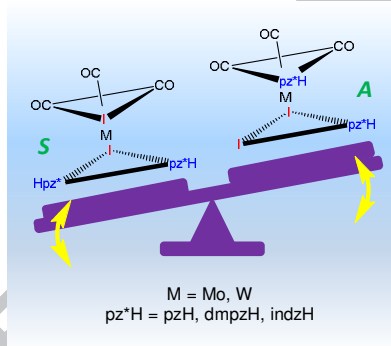
## Synopsis and Pictogram for Preliminary Contents

**Syntheses, solid structures, and behavior in solution of  $[Ml_2(CO)_3(\text{pyrazole})_2]$  complexes (M = Mo, W)**

Paloma Paredes,<sup>a</sup> Fernando Lorenzo,<sup>a</sup> Sonia Bajo,<sup>a</sup> Elena Cuéllar,<sup>a</sup> Carsten Strohmann,<sup>b</sup>  
 Jose M. Martín-Alvarez,<sup>a</sup> Daniel Miguel,<sup>a</sup> and Fernando Villafañe\*<sup>a</sup>

<sup>a</sup> *GIR MIOMeT-IU Cinquima-Química Inorgánica, Facultad de Ciencias, Campus Miguel Delibes, Universidad de Valladolid, 47011 Valladolid, Spain.*

<sup>b</sup> *Anorganische Chemie, Technische Universität Dortmund, Otto-Hahn-Straße 6, 44227 Dortmund, Germany.*



Molybdenum and tungsten heptacoordinated complexes  $[Ml_2(CO)_3(\text{pyrazole})_2]$  have been synthesized and characterized. In solid state they present two possible geometries, either *S* (symmetric) or *A* (asymmetric), with very similar calculated energies. All the complexes are fluxional, each isomer showing a different behavior in solution.

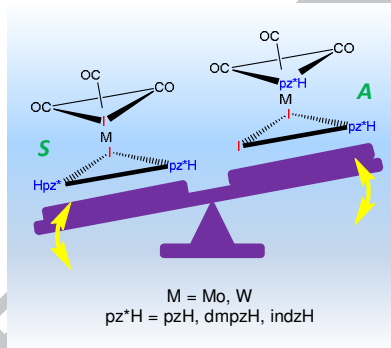
## Synopsis and Pictogram for Preliminary Contents

**Syntheses, solid structures, and behavior in solution of  $[Ml_2(CO)_3(\text{pyrazole})_2]$  complexes (M = Mo, W)**

Paloma Paredes,<sup>a</sup> Fernando Lorenzo,<sup>a</sup> Sonia Bajo,<sup>a</sup> Elena Cuéllar,<sup>a</sup> Carsten Strohmann,<sup>b</sup>  
 Jose M. Martín-Alvarez,<sup>a</sup> Daniel Miguel,<sup>a</sup> and Fernando Villafañe\*<sup>a</sup>

<sup>a</sup> *GIR MIOMeT-IU Cinquima-Química Inorgánica, Facultad de Ciencias, Campus Miguel Delibes, Universidad de Valladolid, 47011 Valladolid, Spain.*

<sup>b</sup> *Anorganische Chemie, Technische Universität Dortmund, Otto-Hahn-Straße 6, 44227 Dortmund, Germany.*



Molybdenum and tungsten heptacoordinated complexes  $[Ml_2(CO)_3(\text{pyrazole})_2]$  have been synthesized and characterized. In solid state they present two possible geometries, either *S* (symmetric) or *A* (asymmetric), with very similar calculated energies. All the complexes are fluxional, each isomer showing a different behavior in solution.